Article ID: 1006-8775(2008) 01-0001-01

NUMERICAL EXPERIMENTS AND ANALYSIS OF DIGITAL FILTER INITIALIZATION FOR WRF MODEL

WANG Shu-chang (王舒畅)[1, 2], HUANG Si-xun (黄思训)[1], ZHANG Wei-min (张卫民)[2], ZHU Xiao-qian (朱小谦)[2], CAO Xiao-qun (曹小群)[2], LI Yi (李　毅)[1]

(1. Institute of Meteorology，PLA University of Science and Technology, Nanjing, 211101 China; 2. School of Computer Science, National University of Defense Technology, Changsha, 410073 China)

ABSTRACT: Initialization and initial imbalance problem were discussed in the context of a three-dimensional variational data assimilation system of the new generation "Weather Research and Forecasting Model". Several options of digital filter initialization have been tested with a rain storm case. It is shown that digital filter initialization, especially diabatic digital filter initialization and twice digital filter initialization, have effectively removed spurious high frequency noise from initial data for numerical weather prediction and produced balanced initial conditions. For six consecutive intermittent data assimilation cycles covering a 3-day period, mean initialization increments and impact on forecast variables are studied. DFI has been demonstrated to provide better adjustment of the hydrometeors and vertical velocity, reduced spin-up time, and improved forecast variables quantity.

Key words: digital filter initialization; assimilation; high frequency oscillations; initial states

CLC number: P433 **Document code:** A

1 INTRODUCTION

The Weather Research and Forecasting (WRF) Model is a new developed non-hydrostatic mesoscale numerical weather prediction system designed to serve both operational forecasting and atmospheric research needs. WRF features multiple dynamical cores, a three-dimensional variational (3D-VAR) data assimilation system, and a software architecture allowing for computational parallelism and system extensibility. WRF makes an operational forecasting model that is flexible and efficient computationally, while offering the advances in physics, numeric, and data assimilation contributed by the research community. In recent years, WRF was widely applied both oversea and at home[1], whereas there is seldom scientific research on the initialization or the initial noise problem which exists in WRF inherently. The veracity and stability of model forecasting can only be afforded with reasonable and consistent initial conditions since formation of the initial states condition is foundation of Numerical Weather Prediction (NWP). The initial model states of WRF were generated by interpolating analyses from global models or large-scale models onto the WRF model grids, which will introduce initial imbalance and rapid model adjustment exciting acoustic and gravity waves that last several hours in the model integrations. Assimilation is to determine as accurately as possible of the actual atmosphere using all available information. WRF 3D-VAR involves observations before launching forecasting, however, the observational data could not really reflect the actual atmospheric states due to the systematic error or instructional error. As what previous researches [2] pointed out, however, the interpolation and the three-dimensional variational assimilation schemes unavoidably introduce imbalances between mass and wind fields to the initial states. Thus the imbalances between wind and mass fields upset the internal dynamical balance of the model and leads to spurious fast oscillations associated with gravity–inertia waves and causes the spin-up phenomenon. To filter out these oscillations, Lynch and Huang [3] have proposed a simple method based on digital filtering that can filter out fast oscillations as efficiently as nonlinear normal mode initialization [4].

Received date: 2007-10-18; **revised date:** 2007-12-14

Foundation item: National Natural Science Foundation of China (40675020)

Biography: WANG Shu-chang, female, native from Hunan Province, Ph.D., mainly undertaking the study on numerical prediction and data assimilation.

E-mail: wangshuchang@126.com

Filtering the optimal initial condition at the end of an MM5 4DVAR may reduce the noise by 20% as shown in De Pondeca and Zou [5]. Digital filter initialization (DFI) can be implemented as a strong constraint by filtering the model fields at the beginning of each forecast or as a weak constraint as described in Gauthier and Thepaut [6]. Chen and Huang [2] tested several configurations of the DFI to the fifth-generation Mesoscale Model (MM5) and assessed the impact of DFI on MM5 forecasts.

This paper is organized as follows. After introducing the WRF and initialization outlined in section 1, basic principles and several configurations of the DFI package of WRF (version 2.1.2) are described briefly in section 2. The experimental setup to determine the noise characteristics caused by interpolations and objective analyses is presented in section 3. In section 4, a heavy rain case is chosen to demonstrate how DFI filters out the noise and improves the dynamic consistency of the model fields, and several measures of the efficacy of the digital filtering scheme in removing gravity-inertia-wave oscillations from the forecast were investigated. Intermittent cycling data assimilation experiments using the same framework are then presented and discussed in section 5. Conclusions and discusses are made finally.

2 DESCRIPTION OF DFI

2.1 *Method of DFI*

The theoretical foundation of DFI is that the high frequencies are removed by applying a digital filter to a short time series generated by an integration from the initial data. Digital filter initialization involves with removing high frequency oscillations from the temporal signal represented by the meteorological fields. A general description of digital filter initialization can be found in Lynch [7].

In order to filter out the high frequencies of a function of time, $x(t)$, with low and high frequency components, one may first calculate the Fourier transform $X(w)$ of $x(t)$; then multiply $X(w)$ by an appropriate weighting function $H(w)$, to eliminate the high frequency components, i.e. to set the coefficients of the high frequencies to zero; with the step function $H(w)$ defined by

$$H(w)=\begin{cases}1, & |w|\le|w_c|;\\ 0, & |w|>|w_c|\end{cases}$$

Time oscillations exceeding a cut-off frequency $\omega_c = 2p/T_c$ can be filtered by applying a digital filter to a time series $x_k = x(t_k)$, for $t_k = k\Delta t$, Δt being the time-step. Calculate the inverse transform finally.

This proceeds by doing a convolution of $x(t)$ with a step function $h(t)$ so that

$$x*h(t_N)=\sum_{k=-\infty}^{+\infty} h_k x_{N-k}$$

The step function h_k is found to be:

$$h_k=\frac{\sin(\omega_c k\Delta t)}{kp}$$

In practice, the convolution is restricted to a finite time interval of time span, T_s:

$$T_s = 2M\Delta t$$

And then we can write the convolution as:

$$x*h(t_0)=\sum_{k=-M}^{M} a_k x_k$$

with $a_k = -h_{-k}$. This truncation introduces 'Gibbs oscillations' which can be attenuated by introducing a Lanczos window. It implies that the weights a_k are defined as:

$$a_k = -h_{-k}W_k$$

with the Lanczos window as $W_k = \dfrac{\sin(kp/(M+1))}{kp/(M+1)}$.

An alternative has been proposed by Lynch[8] to use a Dolph-Chebyshev window in which case

$$W_k=\frac{1}{2M+1}\left[1+2r\sum_{m=0}^{M} T_{2M}(u_0\cos\frac{q_m}{2})\cos mq_k\right]$$

where T_{2M} is the Chebyshev polynomial of degree of $2M$, and $1/u_0=\cos(p\Delta t)/t_s$, $1/r=\cosh(2M\,\mathrm{acosh}\,u_0)$, $q_k=(k2p)/M$. The time span of the window is chosen so that $t_s = M\Delta t$.

In Lynch[8], it is proved that the Dolph window is an optimal filter. Since an optimal filter is, by construction, the best possible solution to minimize the maximum deviation from the ideal in the pass and stop-bands, the Dolph filter shares this property provided that the equivalence holds.

2.2 *DFI for WRF*

In recent years, digital filter initialization (DFI) was pursued actively by the research community and operational centers due to its incomparable advantages, as there is no need to compute or store normal modes or to separate vertical modes. DFI can also meet the need of initializing unanalyzed variables such as cloud water, rainwater, and vertical velocity and the filtered fields of these variables are consistent with the basic dynamic fields. Most importantly, it is applicable to non-hydrostatic models, which is an unavoidable tendency in the development of current NWP.

The continuous advancement of assimilation, rapid updating and analysis system requires shortened assimilation period and quickened frequency of observation data assimilation.

Due to the facility of implementation and maintenance of DFI, a few options of DFI defined by Huang and Yang [9] were applied to WRF(V2.1.2) as available initialization schemes used in this paper.

DDFI (diabatic digital filter initialization) succeed in taking the diabatic processes of the model into account, as the time series of the filtered model variables are produced by a diabatic integration of the model. In order to center the time series at the initial analysis time, an adiabatic backward integration is run first, followed by a diabatic forward integration to produce the time series for the filter. After the filtering, the initialized model state valid at the analysis time is used as the initial state for the final forecast. This is a real initialization scheme, but may have problems due to backward integration. As diabatic processes are basically nonreversible, they were all switched off during the backward integration. This brings some inconstancies to the time series of model state.

TDFI (twice digital filter initialization) is similar to DDFI, but the filter is also applied to the time series from the backward integration. As the filter is applied twice, it requires shorter time integrations.

DFL (digital filter launching) is not really an initialization scheme, as the filtered state is not at the initial time. A short-term forecast is made first to produce a time series of the model state. A digital filer is then applied to the time series to produce a filter model state. The final forecast will be launched from the filtered state. DFL does not need a backward integration and is relatively easy to implement. It removes noise efficiently and should be able to provide noise free background model state for the next data assimilation cycle.

3 DESIGN OF CASE STUDY

3.1 *Method of DFI*

The heavy rain processes chosen for demonstration is a local rainstorm incident that occurred during 0000 UTC 02 July to 1200 UTC 05 July 2006. It was under the main circulation background that a trough moved eastward and became deeper around Baikal area on the 500hPa height field in the prophase of the rainfall, which caused rapid strengthening of the ridge over Xinjiang Region and accumulation of cold air. Therefore, a persistent heavy rainstorm occurring near the Huaihe River basin was brought by the convergence of the moisture and warm air beside the subtropical anticyclone and this cold air. Southwesterly jet at the lower level of 850hPa significantly strengthened up to 12 – 18m/s, which continuously transported water vapor from the Bay of Bengal and South China Sea to Huaihe valley since 2 July. There appeared a shear line along Xi'an to Zhenzhou. Due to the incursion of cold air, a low vortex is spurred around Zhenzhou and severe rainfall happened in the center of the low vortex and on the two sides of the shear line on 3 July.

With the low vortex moving to the east, the shear line became cold and retreated to the south slowly. With the upper air trough moving east into sea, the shear line became weak and then disappeared and accordingly this rainfall process was over.

During 1 – 6 July, the total precipitation of this process reached about 200 – 300mm in the middle and lower reaches of Huaihe River, which negatively affected traffic, agriculture and people's normal livelihood, and even caused the loss of properties and lives.

3.2 *Experimental configuration*

All numerical experiments are performed using the WRF model. The model top is at 50hPa. The center of the simulation domain is located at (115°E, 35°N). The model domain of 144 × 109 grid points uses 15 km horizontal grid spacing and divides into 31 layers with different intervals in the vertical direction. The integration time step is 90 s. The physics package includes WSM3 microphysics, Monin-Obukhov surface scheme, YSU PBL scheme, and Kain-Fritch cumulus parameterization.

A number of simple cold-start runs with different DFI configurations have been performed. For the purpose of representing the impact of objective analysis on initial noise, NODFI experiment is carried using the initial conditions directly from the interpolated global analysis for the WRF 15-km grid without any objective analysis involved. The experiments of all three DFI options with the WRF 3D-VAR are carried out to assess the noise characteristics caused by objective analyses. In these experiments, the Dolph filter is selected, and the cutoff is 1 h (this should filter out oscillations with frequency shorter than 1/1h). The analysis time is at 0000 UTC 02 July 2006, and the filter span is 3 h for DFL, 4 h for DDFI and 2 h for TDFI. Five experiments are performed following the configuration shown in Tab.1.

4 RESULTS AND ANALYSIS

4.1 *Initial noise reduction*

Lynch and Huang[1] proposed the mean absolute surface pressure tendency N,

$$N = \frac{1}{IJ}\sum_{i=I}^{I}\sum_{j=J}^{J}\left|\frac{\partial p_s}{\partial t}\right|_{ij}$$

denoting calculation over the whole model domain as a characteristic quantity that reflects directly the overall balance of the model states. As shown in Fig.1, N of all the three DFI procedure tests are obviously reduced to an reasonable level of about 2 hPa(3h)$^{-1}$,while the un-initialized N is nearly to 10 hPa(3h)$^{-1}$ at the initial time and then drops to around 3 hPa(3h)$^{-1}$ over 6 hours. It is noticeable that the VARNODFI test has much higher noise level than the NODFI test that is without observations, especially in the first ten minutes. It is implied that the dynamic imbalance and noise phenomenon are caused by both vertical interpolation and assimilation analysis.

Tab.1 Analysis and initialization configuration of the experiments

EXPERIMENTS	ANALYSIS	INITIALIZATION	NFILT	TSPAN(h)	CUTOFF(h)
VARNODFI	WRF-3DVAR	-	-	-	-
NODFI	-	-	-	-	-
VARDFL	WRF-3DVAR	DFL	7(DOLPH)	3	1
VARDDFI	WRF-3DVAR	DDFI	7(DOLPH)	4	1
VARTDFI	WRF-3DVAR	TDFI	7(DOLPH)	2	1

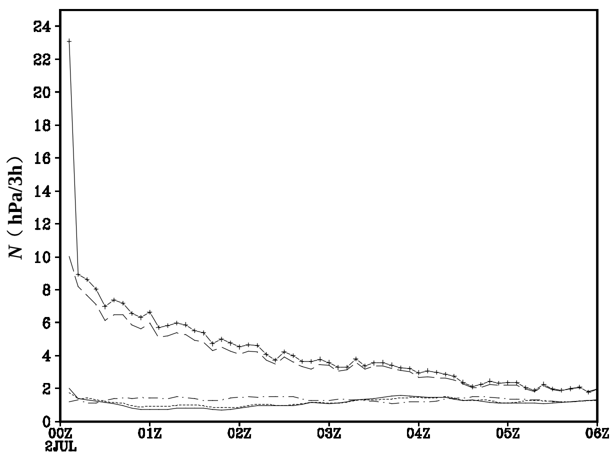

Fig1. The 6 h evolutions of the mean absolute surface pressure tendency N(unit: hPa(3h)$^{-1}$) of five WRF forecasting experiments starting at 0000UTC 2 July 2006.(cross marked line is for VARNODFI, long dash line is for NODFI, dot dash line is for VARDFL, dot line is for VARDDFI, and solid line is for VARTDFI).

Using DFI options, the noise of all the VAR-DFI tests reduce to a lower level especially after the first hour. It is difficult to distinguish the curve of TDFI from the one of DDFI and they are pretty much the same thing.

Following Huang [10], while the surface pressure is sensitive to noise in the sense of vertical integration, the midlevel vertical velocity indicates the internal noise. Digital filter initialization well performed the reduction of noise as demonstrated by the time evolution of the surface pressure and a midlevel vertical velocity at a model grid [10,11]. As shown in Fig.2 and Fig.3, during the first 6 h, high frequency oscillation of un-initialized surface pressure and vertical velocity indicate imbalance in the initial mass and wind fields. However, the amplitude of the oscillations is quite mild in the two forecasts from initialized initial state. Moreover, the initializations using the two DFI options have small differences in their following forecast. In details, the difference is less than 0.1hPa in surface pressure and 0.5 cm/s in the 500-hPa vertical velocity, and the curves of the two forecasts with DDFI and TDFI are similar and it is even impossible to determine which is better.

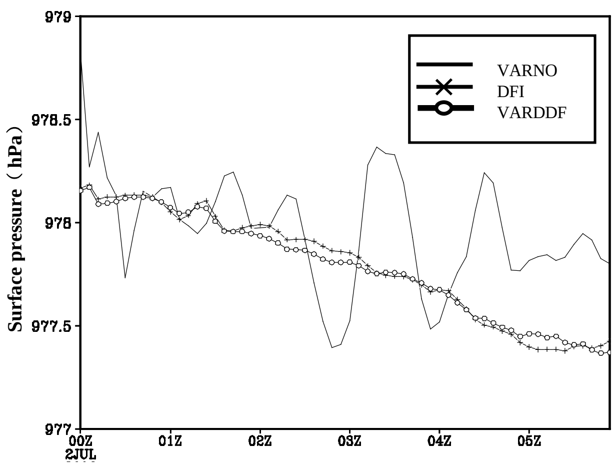

Fig.2 Temporal evolution of surface pressure (unit: hPa) at a model grid located at (126^{o}E, 40^{o}N).

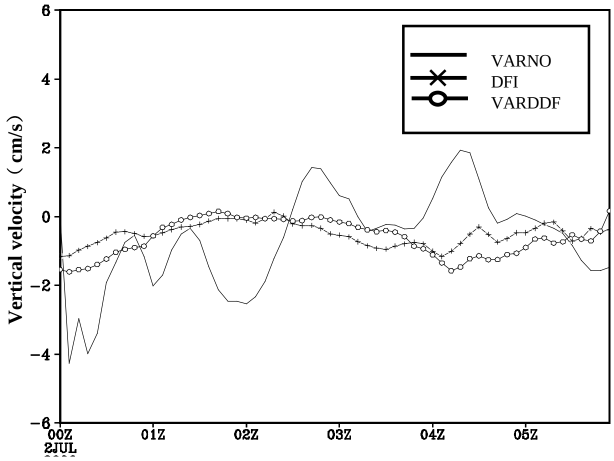

Fig.3 Temporal evolution of vertical velocity（unit: cm/s）on 500 hPa level at the same model grid.

Initial surface pressure tendency (hPa(3h)$^{-1}$) maps of un-initialized analysis and initialized analysis of DDFI, TDFI and DFL are displayed in Fig.4. It is considered that the impact made by digital filter initialization is actually a marginal improvement in reducing the initial noise of the whole domain. Moreover, the intense isolines located at around 34°N in maps of initialized analysis demonstrate that DFI procedures accentuate the region which was characterized by vigorous convective system as the similar pattern shown by the real distribution of initial surface pressure tendency coming from observations.

It is also noticeable in the graph that contours of DFL near the boundary regions are abnormally dense, which may be partly caused by the lack of backward integration, and then lead to less consistence with the actual dynamic fields since the filtered state is not at the initial time.

4.2 *Spin up relief*

As demonstrated by Huang and Sundqvist[12], because the forward integration of diabatic digital filtering initialization includes full physical processes, after initialization, the initial state of hydrometeor fields can be generated while it is unavailable through objective analysis. Moreover it can be more consistent with the mass field and wind field than those without this initialization. Considering as another factor of revealing the effect of an initialization scheme, the domain-averaged precipitation rate is defined to be similar to be the tendency of mean absolute surface pressure to characterize the spin-up feature of the moisture fields. Fig.5 shows the evolutions of domain-averaged precipitation rate PR (mm/day) of three 24-h forecasts in their first 12 h, one is from uninitialized analysis and the other two are from different digital filter initialization options. Clearly the forecast from uninitialized analysis has much larger PR than the other two forecasts during the first eight hours, and its sharp increase from zero to about 18 mm(day)$^{-1}$ within the initial five hours is an pronounced feature. Moreover, precipitation rates of the two initialized forecasts exceed that of the uninitialized one and keep the ascendant across the remaining forecasting of the whole 24 hours. This indicates that the forecast from initialized analysis has larger predicted precipitation than the uninitialized one. And the real precipitation rate derived from every 6 h observations is 11.7955 at 06Z and 13.5468 at 12Z, as shown with solid triangles in Fig.5, which demonstrates that the DFI precipitation forecasting is well coincident with the actual case.

In addition, there is little difference between the conditions of DDFI and TDFI. Although increasing obviously in the early four hours, they both evolve moderately during the whole forecast.

Tab.2 Root mean squares of initialization increments of wind fields, temperature, specific humidity, perturbation pressure and surface pressure averaged in the whole simulating domain at 0000UTC 2 July 2006. (The initialization increment is the difference between the initialized analysis and uninitialized analysis)

Variable	U(m/s)	V(m/s)	T(k)	Q(g/kg)	Pp(hPa)	W(m/s)	PSFC(hPa)
DFL Increment	1.103	1.178	0.668	0.335	0.290	0.061	0.900
DDFI Increment	0.478	0.482	0.342	0.106	0.256	0.029	0.708
TDFI Increment	0.335	0.354	0.237	0.071	0.192	0.027	0.847

Tab.3 Root mean squares of difference in wind fields, temperature, specific humidity, perturbation pressure and surface pressure of uninitialized forecast and initialized forecasts averaged over simulated domain of 24 h forecast from 0000UTC 2 July 2006.

Variable	U(m/s)	V(m/s)	T(k)	Q(g/kg)	Pp(hPa)	W(m/s)	PSFC(hPa)
DFL Difference	2.251	2.224	0.888	0.526	0.454	0.123	0.683
DDFI Difference	2.114	1.985	0.793	0.474	0.332	0.126	0.495
TDFI Difference	2.072	1.945	0.794	0.469	0.328	0.120	0.490

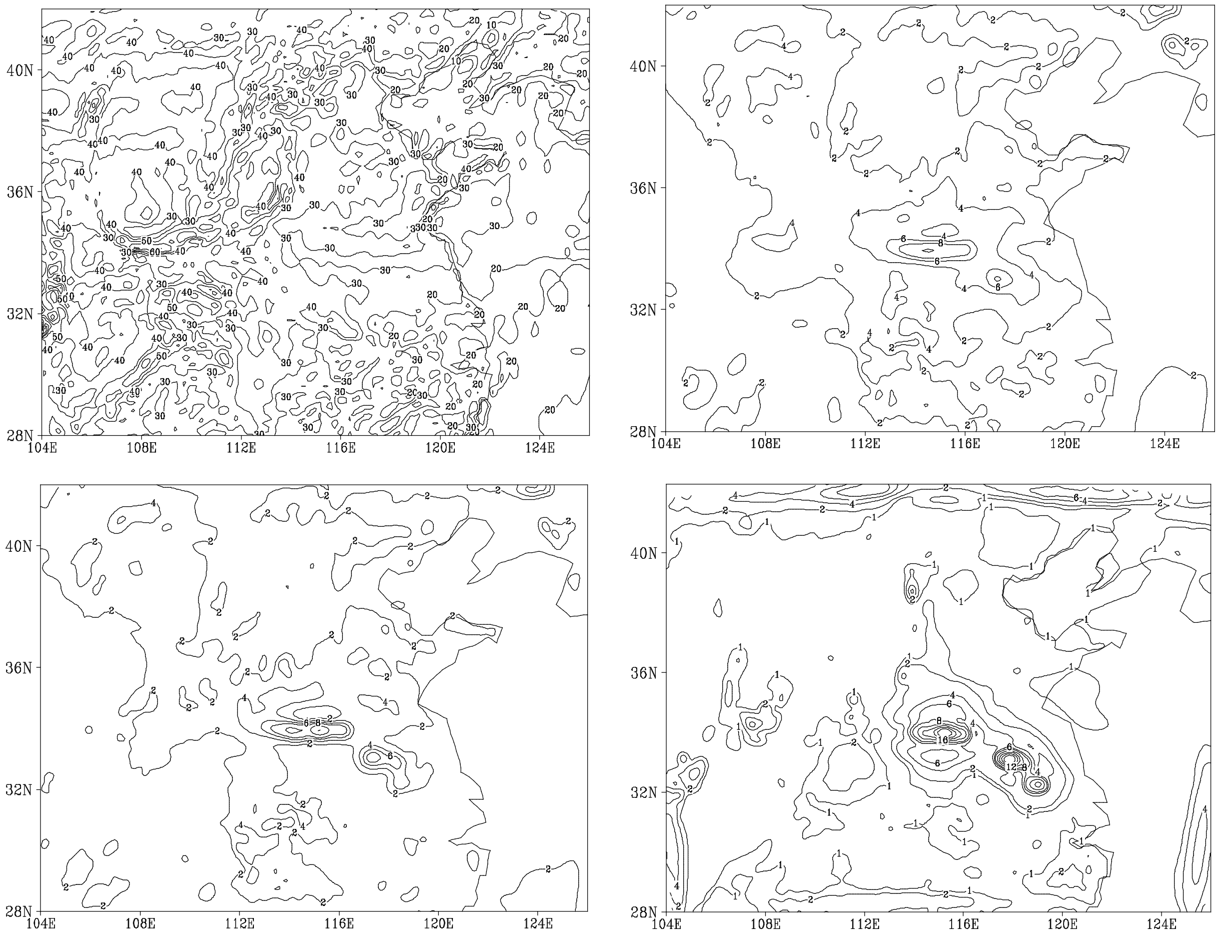

Fig.4 Initial surface pressure tendency of uninitialized analysis (left upper) (the interval is 10 hPa$(3\ h)^{-1}$) and initialized analysis of DDFI (right upper), TDFI(left lower) , DFL(right lower) respectively (The interval of the three initialized analysis are 2 hPa$(3\ h)^{-1}$).

However, DDFI has the mildest increase, which is probably due to the fact that the span of TDFI is shorter than that of DDFI, and longer diabatic forward integration may gain better initial hydrometeor fields and vertical velocity.

Notice that the circumstantiality of the first ten minutes, which is not clear shown in this graph, indicates that the slope of PR from uninitialized analysis is around quintuplicate than those from DDFI and TDFI.

As discussed above, due to DFI procedure, the spin up time is shortened and precipitation rate became larger. It is concluded that the digital filter initialization, whether DDFI or TDFI, has positive impact on relieving the spin-up phenomenon. There is still spin up problem remained, however, longer filter span can be expected to lead to better adjustment of the hydrometeors fields and vertical velocity.

4.3 *Initialization increments*

One of the characteristics essential to any satisfactory initialization procedure is that the changes made to the initial fields are acceptably small. Tab.2 gives the root mean square of initialization increments of some typical variables. It is can be seen that all the initialization increments are reasonablly small and generally less than the observational error or the analysis increments. Rms of DFL increments are much larger than those of the other two initialization options, especially the wind fields, the table numerals of DFL of which are more than twice than those of the DDFI or TDFI. And compared to rms of DDFI increments, rms of the corresponding TDFI increments are quite small.

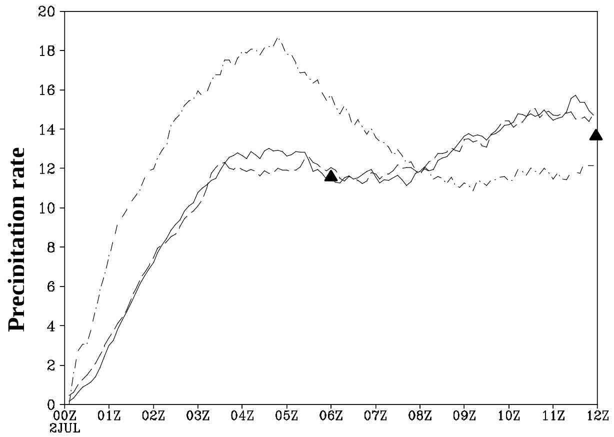

Fig.5 The 12 h evolutions of domain-averaged precipitation rate, PR (unit: mm/day) of WRF-VAR 24 h forecasts from 0000UTC 2 July 2006 (dot line is from the TDFI analysis, broken line is from the DDFI analysis and dot dashed is from the un-initialized analysis),and every 6h precipitation rate of real rain(marked with solid triangle)at the appropriate time.

The spatial distribution of the differences in sea level pressure between initialized analysis and uninitialized analysis at initial time and at the end of 24 h forecast can be seen in Fig.6. All the contour lines have an order not larger than 1 hPa not only at the initial time but also after 24 h. Moreover the large values area of differences at the end of 24 h forecast are located in the rainfall areas.

Using uninitialized forecast as a reference, similar calculations are made for the 24 h initialized forecasts. Results are shown in Tab.3. The table numerals are

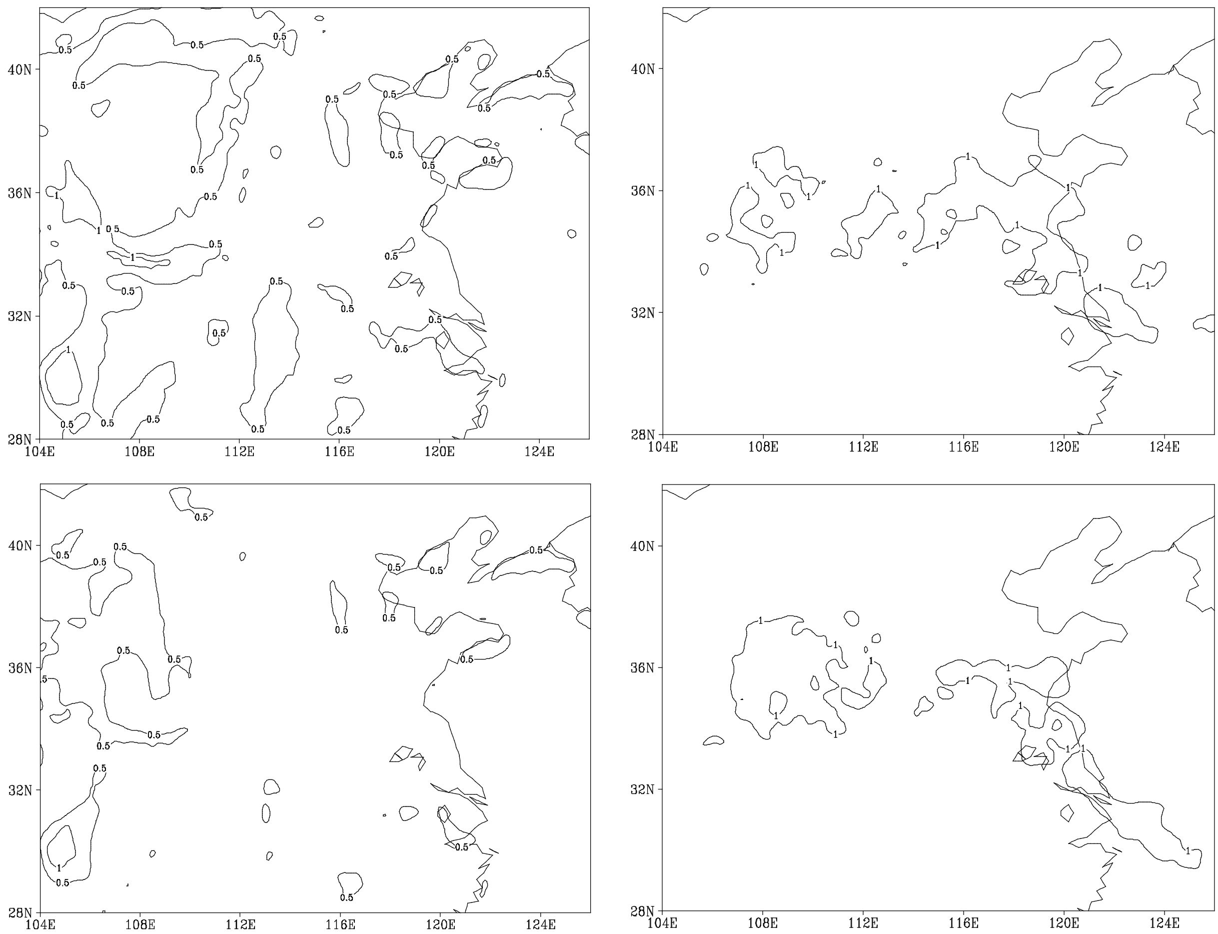

Fig.6 Initialization increment of sea level pressure(unit: hPa) of DDFI (left upper)and TDFI(left lower), difference in sea level pressure between 24 h forecast from the DDFI (right upper) and that from the uninitialized analysis, the same for TDFI (right lower) analysis.

somewhat larger than those of the initial time, but still acceptable. It is suggested that the initialization schemes do not affect the forecasts very much. In addition, it is noticed that difference between the numbers of DFL and the other two DFI options become smaller than those at the initial time. That is to say, during the forecasting integration, impact of different initialization schemes has become neglectable.

5 CYCLING ASSIMILATION FORECASTS

In order to blend information contained in observations originating from different sources with information contained in a prior estimate of the state of the atmosphere referred to as the background state, data assimilation was applied circularly. The analysis increments are built by the assimilation and added to the background state to provide new initial conditions out of which the forecast is made. This process however upsets the internal dynamical balance of the model and leads to spurious fast oscillations associated with gravity–inertia waves.

To evaluate the effect of DFI on forecasts, data assimilation experiments are performed over a 3-day period, from 0000 UTC 02 July to 0000 UTC 05 July2006. Each cycle covers a time span of 12 h and the created analysis is used to make a 24 h forecast. The interpolated NCEP (National Center for Environment Prediction) GFS (Global Forecast System) model state valid at the analysis time is used as the lateral boundaries. The 12-h forecast from the previous cycle is then used as the background for analysis, except at the very beginning of the experiment when the initial model states are obtained by interpolating the GFS model fields. The observation types used in the variational assimilation analysis experiments are described as the following, SYNOP: manual or automatic surface observations from land or ships; PILOT: vertical wind profiles; TEMP: radiosonde balloon ascents from land or ships; AIREP: aircraft observation; SATOB: cloud drift winds from geostationary satellite imagery; TOVS: polar orbiting satellite data.

Three cycling assimilation experiments are designed with the same domain, all physical schemes and time step are the same as the previous experiments. Initializations schemes are DDFI and TDFI, and initialization procedure is applied for every cycling forecasting, the span and cutoff hours are the same as in section 4.

5.1 *Mean initialization increments*

To assess the effect of the DFI procedure on the analysis of cycling assimilation, the mean initialization increments of DDFI and TDFI are shown in Tab.4, which are root-mean-squares (rms) of wind fields, temperature, surface pressure, specific humidity and perturbation pressure vertically integrated over 31 σ-levels and horizontally averaged over the whole model domain. Numbers in Tab. 4 show that initialization increments for both schemes are always reasonably small just as the numbers shown in Tab.3, which indicates that the changes brought by DFI are not swelled by the consecutive assimilation and the following forecast. In general, TDFI has smaller initialization increments than DDFI does.

Tab.4 Root mean squares of initialization increments of wind fields, temperature, specific humidity, perturbation pressure and surface pressure averaged for the six cycling assimilation forecasts.(The initialization increment is the difference between the initialized analysis and uninitialized analysis)

Variable	U(m/s)	V(m/s)	T(k)	Q(g/kg)	Pp(hPa)	W(m/s)	PSFC(hPa)
DDFI Increment	1.554	1.480	0.685	0.414	0.287	0.066	0.725
TDFI Increment	1.465	1.406	0.597	0.387	0.289	0.064	0.810

5.2 *Forecast verification*

To have an idea about the impact of initialization schemes on the forecast quality, three-dimensional model fields generated by a 24-h forecast in every data assimilation cycle are verified against NCEP re-analysis data fields at 0000 and 1200 UTC.

Fig.7 presents the vertical profiles of root mean square (rms) difference between model variables and re-analysis data averaged over the six assimilation forecast cycles. The verified forecasted elements are chosen as temperature, wind, and relative humidity at conventional pressure levels. Considering forecast performance at initial time and 24 h forecast, the rms profiles of DFI experiments for both analysis methods are quite similar to those of uninitialized experiments.

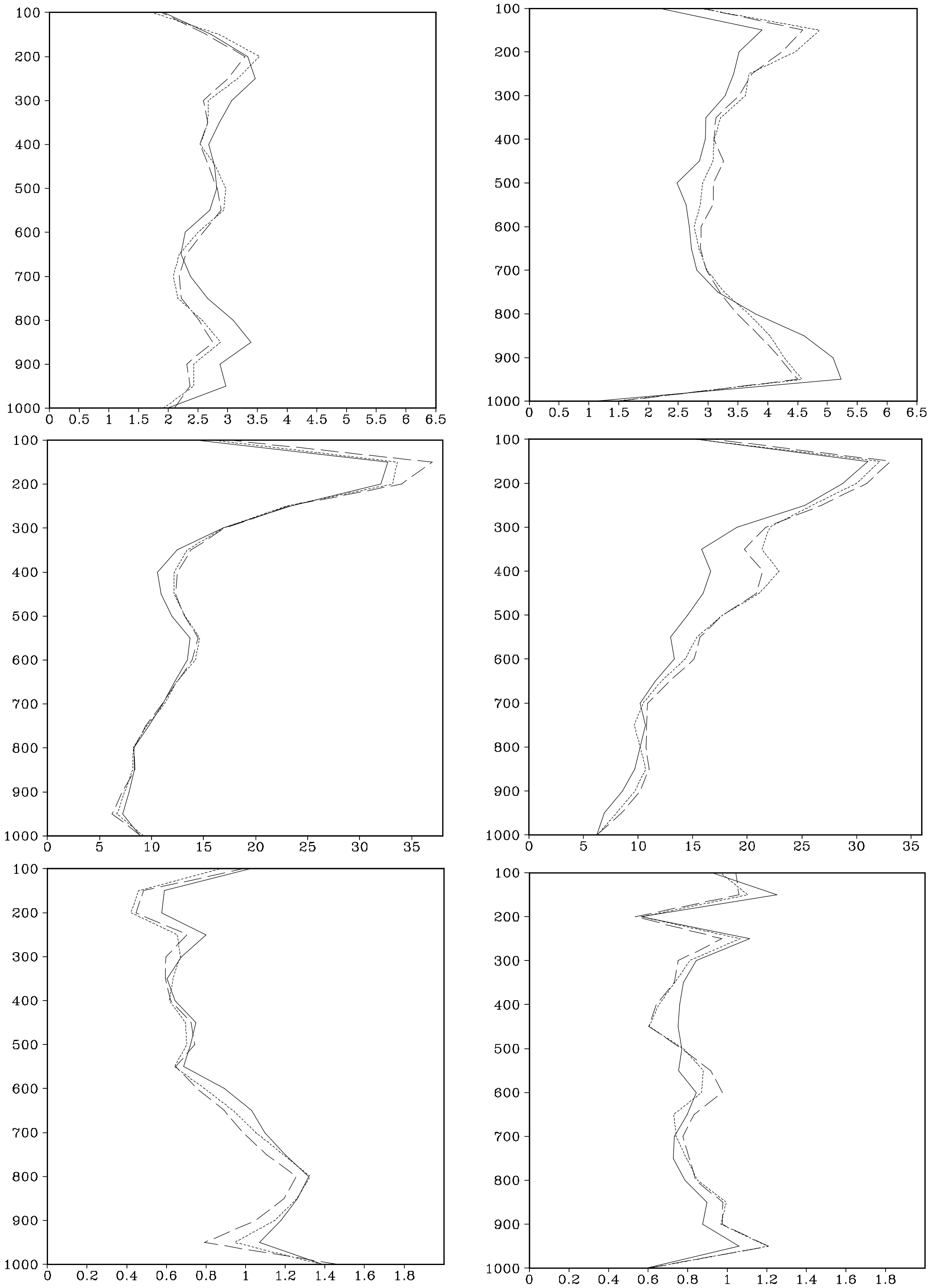

Fig.7 Vertical profiles of root mean square of differences in temperature(upper), relative humidity (middle) and wind fields (lower) between analyses at *t*=0 h (left) and forecasts at t=24 h(right) and NCEP re-analysis data, averaged over 6 consecutive cycles started on 0000 UTC 02 July 2006(solid line is from the un-initialized analysis, broken line is from the DDFI analysis and dot dashed is from the TDFI analysis).

Tab.5 Root mean square of difference in 2-m temperature, 10-m wind, 2-m relative humidity, and sea level pressure between re-analysis real data and 24 h forecast from uninitialized analysis, DDFI and TDFI analysis averaged over the six cycling forecasts cold started on 0000 UTC 02 July

Variables	0000UTC			0600UTC			1200UTC			1800UTC		
	-	DDFI	TDFI	-	DDFI	TDFI	-	DDFI	TDFI	-	DDFI	TDFI
T2m(k)	1.463	1.372	1.408	2.203	2.050	2.025	1.386	1.384	1.385	1.766	1.839	1.846
U10m(m/s)	2.017	1.909	1.878	1.378	1.383	1.393	1.649	1.805	1.796	1.482	1.613	1.667
V10m(m/s)	1.672	1.695	1.735	1.504	1.526	1.537	1.627	1.806	1.817	1.711	1.822	1.845
Q2m(kg/kg)	1.655	1.781	1.863	2.512	2.499	2.521	2.996	2.853	2.855	1.678	1.619	1.641
slvl (Pa)	1.351	1.260	1.512	0.730	0.716	0.716	0.615	0.630	0.617	0.809	0.805	0.804

Surface model fields are also verified every 6 h as shown in Tab.5. For the rms at each time of 2-m temperature, 10-m wind, 2-m relative humidity and sea level pressure, the differences in scores averaged over the six cycling forecasts from DFI analysis and uninitialized analysis are generally insignificant.

As described above, it is concluded that DFI procedure performs satisfactorily and does not degrade the forecasts of these selected predicted variables.

6 SUMMARY

A storm rain case study and intermittent data assimilation experiments are implemented to assess the impact of DFI on WRF model forecasts in this paper. Digital filtering has been shown to effectively remove the high frequency noise and produce a balanced initial model state. It is also shown that DFI has positive impact on relieving the spin-up phenomenon, shortening the spin-up time for precipitation, leading to larger forecasting precipitation. Statistics of all the experiments of initialization increments and the differences of forecast made by DFI are acceptably small. Results of investigation of the connective assimilation forecasts with initialization indicate that DFI works satisfactorily and does not degrade the forecasts of the selected predicted variables.

As possessing all the three characteristics is essential to any satisfactory initialization procedure advanced by Lynch [3], DFI has been considered to be a simple and effective means of initializing data for numerical weather prediction. In recent years, initial condition and parameters can be identified in four–dimensional variational assimilation (4D-VAR) using the adjoint method [13-15], which is one of the leading fields in atmospheric science and physical oceanography. From a long-term point of view, use of the digital filter is not restricted to initialization; it may also be implemented as a weak constraint penalizing the analysis towards a balanced state in WRF 4D-VAR system following closely Polavarapu[16] and Wee[17] in the near future. Impact of DFI as a weak constraint on WRF 4D-Var forecasts of severe weathers will be under investigation.

REFERENCES:

[1] WANG Shu-chang, HUANG Si-xun, LI Yi, Sensitive numerical simulation and analysis of rainstorm using nested WRF model. [J]. J. Hydrodyn., Ser.B, 2006, 18(5): 578-586.
[2] CHEN Min, HUANG X Y. Digital filter Initialization for MM5 [J]. Mon. Wea. Rev., 2006,134(4): 1222-1236.
[3] LYNCH P, Huang X Y. Initialization of the HIRLAM model using a digital filter [J]. Mon. Wea. Rev., 1992, 120(6), 1019-1034.
[4] MACHENHAUER B. On the dynamics of gravity oscillations in a shallow water model with applications to normal mode initialization [J]. Beitr. Atmos. Phys., 1977, 50: 253-271.
[5] DE PONDECA M S F V, ZOU X. Moisture retrievals from simulated zenith delay "observations" and their impact on short-range precipitation forecasts [J]. Tellus, 2001, 53A(2): 192-214.
[6] GAUTHIER P, THEPAUT J N. Impact of the digital filter as a weak constraint in the preoperational 4DVAR assimilation system of Météo-France [J]. Mon. Wea. Rev., 2001, 129(8), 2089-2102.
[7] LYNCH P. Digital filters for numerical weather prediction. HIRLAM [R] Technical Report. 1993, No 10.
[8] LYNCH P. The Dolph-Chebyshev window: a simple optimal filter [J]. Mon. Wea. Rev., 1997, 125(4): 655-660.
[9] HUANG X Y, LYNCH P. Diabatic digital filter initialization: Application to the HIRLAM model [J]. Mon. Wea. Rev., 1993, 121: 589-603.
[10] TEMPERTON C, WILLIAMSON D L. Normal-mode initialization for a multilevel gridpoint model. Part 1: Linear aspects [J]. Mon. Wea. Rev., 1981, 109(4): 729-743.
[11] WILLIAMSON D L, TEMPERTON C. Normal-mode initialization for a multilevel gridpoint model. Part II: Nonlinear aspects [J]. Mon. Wea. Rev., 1981, 109(4): 744-757.
[12] HUANG X Y, SUNDQVIST H. Initialization of cloud water content and cloud cover for numerical prediction models [J]. Mon. Wea. Rev., 1993, 121(10): 2719-2726.
[13] WAN Qi-Lin, XUE Ji-shan, CHEN Zhi-tong, et al. The test of applying radar TREC wind in three-dimensional variational assimilation [J]. J. Trop. Meteor., 2006, 12(1): 59-66.
[14] DU Qin, SHEN Tong Li. Study of modification to model error by using the adjoint model assimilation system [J]. J. Trop. Meteor., 2007, 23(2): 182-188.
[15] GU Jian-feng, XUE Jishan, YAN Hong. A summarization of the four- demensional variational Doppler radar analysis system[J]. J. Trop. Meteor., 2004, 20(1): 2-14.
[16] POLAVARAPU S, TANGUAY M, Fillion L. Four dimensional variational data assimilation with digital filter initialization [J]. Mon. Wea. Rev., 2000, 128(7): 2491-2510.
[17] WEE T K, KUO Y H. Impact of a digital filter as a weak constraint in MM5 4DVAR [J]. Mon. Wea. Rev., 2004, 132(2): 543-559.